Frontiers in Heat and Mass Transfer (FHMT), 16, 6 (2021)
DOI: 10.5098/hmt.16.6

Global Digital Central
ISSN: 2151-8629

Frontiers in Heat and Mass Transfer

Available at www.ThermalFluidsCentral.org

# EFFECT OF MODIFIED FLY ASH PREPARED BY CATALYTIC COMBUSTION FURNACE ON $Ca^{2+}$ AND $Mg^{2+}$ IN WATER

Hongjun Wang*, Shihong Zhang

*School of Environment and Energy Engineering, Beijing University of Civil Engineering and Arch., Beijing, 100044, China*

## ABSTRACT

Catalytic combustion can inhibit the formation of CO and $NO_x$, and greatly reduce the concentration of unburned alkanes. The hardness of tap water in Beijing is too high. In order to test whether the modified fly ash can reduce its hardness, clay, shale and fly ash bricks were prepared by catalytic combustion furnace. The results show that the fly ash brick has a great influence on $Ca^{2+}$ and $Mg^{2+}$ in water, increasing $Ca^{2+}$ concentration by 59.96% and decreasing $Mg^{2+}$ concentration by 41.22%. Thus modified fly ash could not reduce hardness of water but could be used as an $Mg^{2+}$ adsorbent.

**Keywords**: *Catalytic combustion; Fly ash; Hardness of water; $Ca^{2+}$; $Mg^{2+}$*

## 1. INTRODUCTION

Fly ash is tiny ash particles discharged during the combustion of fuel (mainly coal), which can cause air pollution and endanger human health without treatment. In 2018, the industries with the largest production of fly ash in China were power and heat production and supply industries, followed by chemical raw materials and chemical products manufacturing, non-ferrous metal smelting and rolling processing industries, petroleum, coal and other fuel processing industries, paper and paper products (Ministry of Ecological Environment of the People's Republic of China., 2020).

The comprehensive utilization market for fly ash is very broad. In the field of construction, concrete mixed with an appropriate proportion of fly ash has good compressive strength and axial tensile strength (Zhou *et al.*, 2019), and the critical strength of frost resistance is also improved (Chen, 2019). Fly ash is composed of a variety of particles, of which irregular glass is one of the more particles in fly ash, mostly composed of spherical and non-spherical aggregates with different roundness. The porous glass body is shaped like a honeycomb, has a large surface area, is easy to adhere to other debris, and the ash contains substances with strong adsorption capacity such as $Al_2O_3$ and $SiO_2$, so the main mechanism of fly ash in water treatment is adsorption. Moreover, modified fly ash is a good adsorbent, which can adsorb not only phosphorus (Zhang *et al*., 2019) but also heavy metal ions such as $Cr^{6+}$, $Cu^{2+}$, $Cd^{2+}$, $Pb^{2+}$ and $As^{3+}$ (Liu, 2008; Luo *et al*., 2020; Huang *et al*., 2020; Kobayashi *et al*., 2020; Medina-Ramirez *et al*., 2019). Modified fly ash can even adsorb Hg (Kuncoro *et al*., 2013). Clay bricks containing an appropriate amount of fly ash have a good compressive strength, and the glazed bricks made from this material are of excellent quality and high aesthetic value (Zhang and Xu, 2020), and have been used in establishing cultural heritage and repairing historic buildings. Calcium is an important component of the plant cell wall and intercellular layer, and plays an important role in regulating the balance of physiological activities in plants. Magnesium participates in numerous physiological activities of plants, including photosynthesis, activation of enzymes and synthesis of nucleic acids and proteins. Deficiency in Mg affects crop yield and quality (Chen *et al*., 2017).

The hardness of water mainly depends on the content of $Ca^{2+}$ and $Mg^{2+}$. Groundwater is the main source of tap water in a considerable part of Beijing. Because of the area's geological structure, the hardness of groundwater is relatively high. Water with high hardness tastes astringent even after boiling. There is no conclusive evidence that scale will do harm to the human body; however, scale does affect some equipment such as boilers, heat exchangers and water heaters. The main reason for scale formation in boilers is that the feed water contains hardness components. After continuous evaporation and concentration at high temperature and high pressure, a series of physical and chemical reactions take place in the boiler, and finally a hard and dense scale is formed on the heating surface. The thermal conductivity of scale is extremely poor. In order to retain the efficiency of the boiler, it is necessary to raise the temperature of fire side, leading to a waste of energy. At the same time, uneven heating of the boiler causes local overheating and can easily damage the boiler. Cleaning scale is not an easy task, and the equipment must stop running when it is cleaned, which will have an impact on daily activities. If the hardness of water can be reduced, the frequency of the cleaning of scale can be reduced.

After being treated at a high temperature, fly ash has an impact on $Ca^{2+}$ and $Mg^{2+}$ in water. This study aimed to explore whether the hardness of water can be reduced by modifying fly ash, clay and shale. The development of the world energy economy is inseparable from fossil fuel (Groll., 2020). Natural gas is widely used in industry (Cao e*t al.*, 2019) as a clean fossil fuel with low pollution emissions during combustion. Natural gas catalytic combustion technology has attracted considerable attention as a means of environmental protection and energy saving (Dopont *et al*., 2001). Three kinds of materials (clay, shale and fly ash) were selected, and the small bricks made of these three materials were prepared by catalytic combustion furnace.

* *Corresponding author. Email: 2108521318097@stu.bucea.edu.cn*

Global Digital Central
ISSN: 2151-8629

## 2. MATERIALS AND METHODS

### 2.1 Main materials

Clay used in the experiment came from Mentougou District of Beijing, fly ash was taken from raw coal produced in Huaibei City of Anhui Province, and tap water was from Chegongzhuang, Xicheng District of Beijing. Deionized water was used in the process of preparing bricks. An analysis of the main components of shale and fly ash is shown in Table 1.

**Table 1** Composition of shale and fly ash.

| *Component* | *$SiO_2$* | *$Al_2O_3$* | *$Fe_2O_3$* | *CaO* | *$K_2O$* | *$Na_2O$* | *MgO* | *$TiO_2$* |
|---|---|---|---|---|---|---|---|---|
| Shale | 55.21% | 30.02% | 2.67% | 1.48% | 3.37% | 0.11% | 1.48% | — |
| Fly ash | 58.24% | 27.46% | 2.86% | 2.11% | 1.41% | 0.35% | 0.95% | 1.27% |

### 2.2 The catalytic combustion furnace system

The catalytic combustion furnace system is illustrated in Fig. 1. The system includes five main parts: gas flow control, water circulation, burner, furnace (including temperature measurement) and exhaust analysis. Before starting the catalytic combustion furnace, all components were checked and the flue gas analyzer was switched on after confirming that there were no problems. The system takes 30 minutes for self-calibration. Then the circulating water pump is started, and the burner is cooled throughout the experiment to avoid the burner cavity temperature being too high to affect the performance. The air flow rate was set to 3.7 $m^3$/h and the natural gas flow rate to 5.0 L/min, and ignited immediately. At this time, the catalyst surface is burnt. Then, the flame is gradually extinguished and the catalyst begins to turn red. When the catalyst had turned completely red, the air flow rate was adjusted to 5.7 $m^3$/h, after which the catalyst surface appeared bright red and the combustion gradually stabilized (Fig. 2). After closing the door of the furnace, the excess air coefficient during complete combustion is given as follows (Liu and Liu, 2009):

$$\alpha = \frac{21}{21 - 79\dfrac{r'_{O_2}}{100 - \left(r'_{RO_2} + r'_{O_2}\right)}} \tag{1}$$

where $r'_{O_2}$ is the volume fraction (%) of oxygen in dry flue gas, and $r'_{RO_2}$ is the volume fraction (%) of triatomic gas in dry flue gas. Both components are measured by flue gas analysis. The excess air coefficient was maintained at slightly more than 2.0 and flow regulation of air and natural gas was determined based on the excess air coefficient.

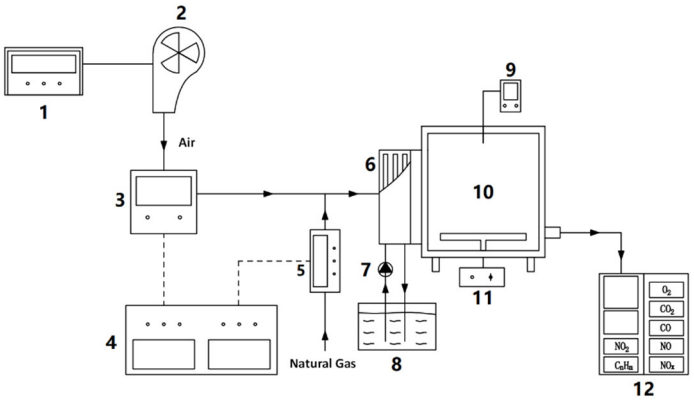


1, Frequency converter; 2, Air pump; 3, Flowmeter 1 (measuring air flow); 4, Adjustable voltage and current stabilizing power supply; 5, Flowmeter 2 (measuring natural gas flow); 6, Burner; 7, Water circulating pump; 8, Water tank; 9, Thermocouple thermometer; 10, Furnace; 11, Speed control; 12, Exhaust gas analyzer

**Fig. 1** The catalytic combustion furnace system

**Fig. 2** Steady state of catalytic combustion

**Table 2** Components of natural gas

| *Component* | *$CH_4$* | *$C_2H_6$* | *$C_3H_8$* | *$N_2$+Ar* | *$CO_2$* |
|---|---|---|---|---|---|
| Volume fraction (%) | 92.83 | 4.69 | 0.49 | 0.48 | 0.92 |

Beijing pipeline natural gas whose components are shown in Table 2 based on volume is used as fuel for firing bricks. Curves of emissions in the exhaust gas of the catalytic combustion furnace are shown in Fig. 3. The main pollutants in exhaust gas are CO and NO, along with a very small amount of $NO_2$. The exhaust gas also contains unburned $CH_4$. The gas concentration of CO increased within the period 0–10 minutes, reached the maximum value of 33.32 mg/$m^3$ in the 10th minute, then decreased, and returned to zero in the 110th minute. The gas concentration of NO generally increased within the period 0–45 minutes, reached the maximum value of 33.24 mg/$m^3$ in the 45th minute, began to decrease in the 55th minute, and returned to zero in the 90th minute. The maximum concentration of $NO_2$ was 1.89 mg/$m^3$ in 45–50 minutes, and it was zero at other times. The concentration of $CH_4$ increased in the period 0–10 minutes, reached the maximum value of 26.92 mg/$m^3$ in the 10th minute, then decreased and returned to zero in the 40th minute. The catalytic combustion furnace was able to realize low pollution emission after heating up for 110 minutes. Sufficient $O_2$ and high temperature cause the formation of thermal NO (Qi *et al.*, 2017). However, the temperature of catalytic combustion is not enough to form a large amount of thermal NO.

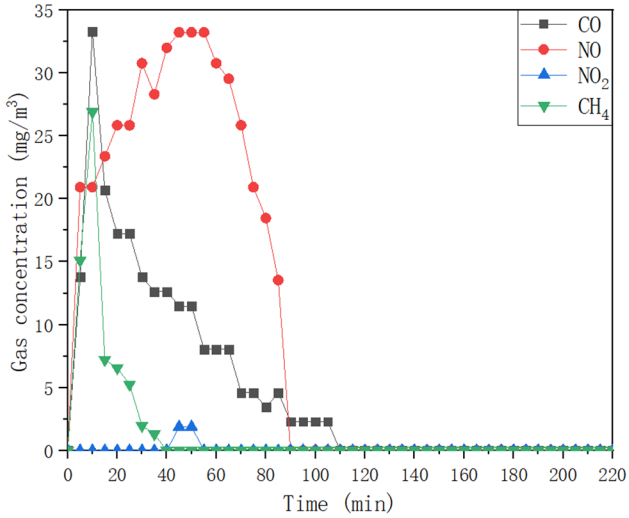


**Fig. 3** Curves of emissions in exhaust gas

### 2.3 Analysis and test instrument

Concentrations of $Ca^{2+}$ and $Mg^{2+}$ were measured by a Thermo Fisher SCIENTIFIC iCAP7000 inductively coupled plasma emission spectrometer, whose structure is shown in Fig. 4. The inductively

Global Digital Central
ISSN: 2151-8629

coupled plasma emission spectrometer is mainly composed of five parts: light source (heat source), sample introduction system, monochromatic system, detection system and computer data processing system. The working principle of the instrument is that the sample is atomized by carrier gas (Ar), then enters the axial channel of plasma in the form of aerosol, and is fully evaporated, atomized, ionized and excited at high temperature in an inert atmosphere, and the characteristic spectral lines of the elements contained are emitted. According to the existence of characteristic spectral lines, identify whether the sample contains certain elements (qualitative analysis) and determine the content of the corresponding elements in samples according to the intensity of characteristic spectral lines (quantitative analysis).

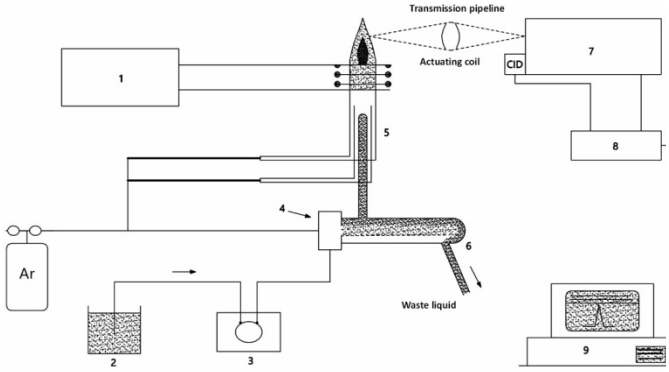


1, High-frequency generator; 2, Sample; 3, Peristaltic pump; 4, Atomizer; 5, Plasma torch; 6, Spray chamber; 7, Spectroscopic system (purged by argon); 8, Microprocessor and control circuit; 9,Computer

**Fig. 4** Schematic diagram of inductively coupled plasma emission spectrometer

## 2.4 Preparation of clay brick, shale brick and fly ash brick by high temperature sintering

The water used to prepare bricks is deionized water to avoid affecting the experimental results because extra $Ca^{2+}$ and $Mg^{2+}$ will be included if tap water is used. The clay, shale and fly ash were first crushed separately and then mixed into a viscous state with deionized water. Next, naturally airing in a formative state, small bricks were produced in a mold with a length of 50 mm, a width of 30 mm and a thickness of 5 mm, and then they were aired for 48 h to ensure that they were completely dry. Fly ash, shale and clay were each prepared into three bricks (giving a total of nine bricks). The bricks were then sintered to 900°C in catalytic combustion furnace according to the specific temperature curve in Fig. 5. The specific temperatures were shown in Table 3. When the furnace is cooled to room temperature (this process usually takes 24 hours), the bricks were removed.

**Table 3** Time and temperature

| *Time(min)* | 0 | 5 | 10 | 15 | 20 | 25 | 30 |
|---|---|---|---|---|---|---|---|
| *Temperature(℃)* | 208 | 352 | 338 | 305 | 321 | 341 | 405 |
| *Time(min)* | 35 | 40 | 45 | 50 | 55 | 60 | 65 |
| *Temperature(℃)* | 438 | 459 | 512 | 543 | 609 | 636 | 656 |
| *Time(min)* | 70 | 75 | 80 | 85 | 90 | 95 | 100 |
| *Temperature(℃)* | 685 | 704 | 719 | 730 | 742 | 753 | 759 |
| *Time(min)* | 105 | 110 | 115 | 120 | 125 | 130 | 135 |
| *Temperature(℃)* | 766 | 772 | 776 | 796 | 803 | 809 | 815 |
| *Time(min)* | 140 | 145 | 150 | 155 | 160 | 165 | 170 |
| *Temperature(℃)* | 818 | 835 | 844 | 853 | 859 | 864 | 865 |
| *Time(min)* | 175 | 180 | 185 | 190 | 195 | 200 | 205 |
| *Temperature(℃)* | 872 | 876 | 879 | 882 | 886 | 889 | 892 |
| *Time(min)* | 210 | 215 | 220 | | | | |
| *Temperature(℃)* | 896 | 898 | 900 | | | | |

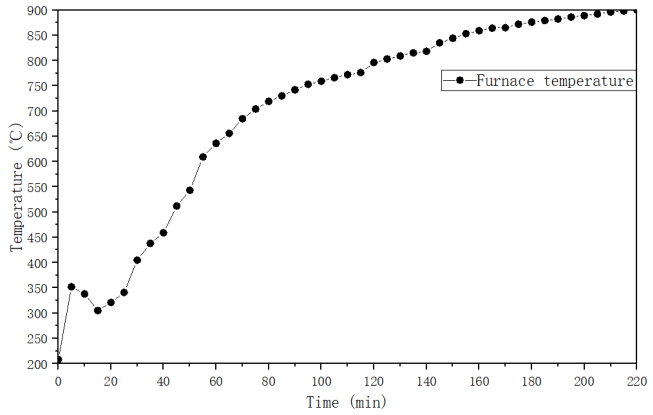


**Fig. 5** Increase curve of furnace temperature

## 2.5 Method

### 2.5.1 Sample control method

The prepared bricks were ground into powder, thus obtaining powder of fly ash, shale and clay. Six 50-mL test tubes each received 5 g of fly ash, clay or shale powder weighed with an electronic balance to a precision of 0.1 mg (two replicates per powder). No powder was added to a seventh test tube as a blank control group. Tap water from Chegongzhuang, Xicheng District, Beijing, was added to the seven test tubes, then the test tube was shaken well until the liquid in test tubes appeared turbid. The seven test tubes were left to stand for 24 hours and the powder settled on the bottom of the tube, as shown in Fig. 6 (a). Thirty milliliters of liquid was then removed from the tube by syringe and filtered through 0.45-μm microporous membranes into a 20-mL test tube. This produced seven filtered samples as shown in Fig. 6(b).

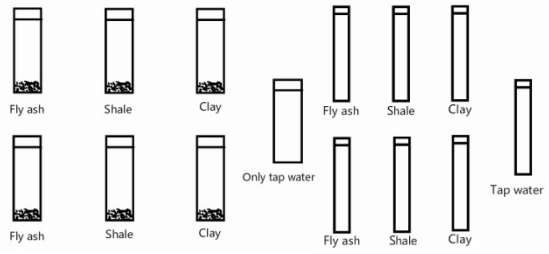


**Fig. 6** (a) Samples before filtration (b) Samples after filtration

### 2.5.2 Standard deviation

According to JJF 1059.1-2012, the experimental standard deviation ( $s(x_k)$ ) of a single measured value $x_k$ in $n$ measurements can be calculated according to Bessel's formula (2):

$$s(x_k)=\sqrt{\frac{\sum_{i=1}^{n}(x_i-\bar{x})^2}{n-1}} \tag{2}$$

where $x_i$ is the measured value of the $i$-th measurement, and $\bar{x}$ is the arithmetic means of a group of measuring values obtained from $n$ measurements.

The experimental standard deviation of the arithmetic ($s(\bar{x})$) mean value $\bar{x}$ of $n$ measurements can be calculated according to Formula (3):

$$s(\bar{x})=\frac{s(x_k)}{\sqrt{n}} \tag{3}$$

## 3. RESULTS

The mass concentrations of $Ca^{2+}$ and $Mg^{2+}$ of seven samples in Fig. 6(b) were measured with the inductively coupled plasma emission spectrometer described previously (Table 4).

**Table 4** The mass concentration of $Ca^{2+}$ and $Mg^{2+}$ in the seven samples after filtration (Fig. 6(b))

| *Mass concentration (mg/L)* | *Fly ash* | *Fly ash* | *Shale* | *Shale* | *Clay* | *Clay* | *Tap water* |
|---|---|---|---|---|---|---|---|
| $Ca^{2+}$ | 184.406 | 185.252 | 126.621 | 125.458 | 120.757 | 121.447 | 115.547 |
| $Mg^{2+}$ | 22.262 | 23.12 | 34.496 | 35.142 | 39.14 | 39.002 | 38.604 |

The arithmetic mean values of the first measurement and the second measurement of clay, fly ash and shale are shown in Table 5.

**Table 5** Average mass concentrations of $Ca^{2+}$ and $Mg^{2+}$

| *Average mass concentration (mg/L)* | *Fly ash* | *Shale* | *Clay* |
|---|---|---|---|
| $Ca^{2+}$ | 184.829 | 126.0395 | 121.102 |
| $Mg^{2+}$ | 22.691 | 34.819 | 39.071 |

According to Formulas (2) and (3), $s(x_k)$ and $s(\overline{x})$ of the influence of clay, shale and fly ash on $Ca^{2+}$ and $Mg^{2+}$ are shown in Table 6.

**Table 6** Standard deviation of average mass concentration of $Ca^{2+}$ and $Mg^{2+}$ in fly ash, shale and clay

| *Standard deviation* | *$Ca^{2+}$* | | | *$Mg^{2+}$* | | |
|---|---|---|---|---|---|---|
| | *Fly ash* | *Shale* | *Clay* | *Fly ash* | *Shale* | *Clay* |
| $s(x_k)$ | 0.822365 | 0.822365 | 0.487904 | 0.606698 | 0.456791 | 0.097581 |
| $s(\overline{x})$ | 0.5815 | 0.5815 | 0.345 | 0.429 | 0.323 | 0.069 |

Because of the systematic error in the measurement, the two measurements cannot be completely consistent, but the values are repetitive and unidirectional. Therefore, the arithmetic mean value can be approximately regarded as the true value, and the relative error can be obtained using the following formula:

$$\delta = \frac{\Delta}{L} \times 100\% \tag{4}$$

where $\Delta$ is the absolute error, obtained by subtracting the true value from the measured value, and $L$ is the true value, which is approximately replaced by the mean value. The results are presented in Table 7.

**Table 7** Relative errors of $Ca^{2+}$ and $Mg^{2+}$ mass concentrations

| *Relative error* | *Fly ash* | *Fly ash* | *Shale* | *Shale* | *Clay* | *Clay* |
|---|---|---|---|---|---|---|
| $Ca^{2+}$ | −0.23% | 0.23% | 0.46% | −0.46% | −0.28% | 0.28% |
| $Mg^{2+}$ | −1.89% | 1.89% | −0.93% | 0.93% | 0.18% | −0.18% |

Table 7 shows that the errors are between −2% and +2%. The rate of change in the $Ca^{2+}$ mass concentration was calculated by Formula (5):

$$\eta_{Ca^{2+}} = \frac{\rho'_{Ca^{2+}} - \rho_{Ca^{2+}}}{\rho_{Ca^{2+}}} \times 100\% \tag{5}$$

where $\rho'_{Ca^{2+}}$ is the concentration of $Ca^{2+}$ in tap water with powder of fly ash, shale and clay (mg/L), and $\rho_{Ca^{2+}}$ is the concentration of $Ca^{2+}$ in tap water without powder (mg/L).

The rate of change in the $Mg^{2+}$ mass concentration was calculated as follows:

$$\eta_{Mg^{2+}} = \frac{\rho'_{Mg^{2+}} - \rho_{Mg^{2+}}}{\rho_{Mg^{2+}}} \times 100\% \tag{6}$$

where $\rho'_{Mg^{2+}}$ is the concentration of $Mg^{2+}$ in tap water with powder of fly ash, shale and clay (mg/L), and $\rho_{Mg^{2+}}$ is the concentration of $Mg^{2+}$ in tap water without powder (mg/L).

The mass concentration change rates of $Ca^{2+}$ and $Mg^{2+}$ calculated by Formulas (5) and (6) are shown in Table 8.

**Table 8** Rate of change in the mass concentration of $Ca^{2+}$ and $Mg^{2+}$

| *Mass concentration change rates (%; + For increase, − for decrease)* | *Fly ash* | *Fly ash* | *Shale* | *Shale* | *Clay* | *Clay* | *Tap water* |
|---|---|---|---|---|---|---|---|
| $Ca^{2+}$ | +59.59 | +60.33 | +9.58 | +8.58 | +4.51 | +5.11 | 0 |
| $Mg^{2+}$ | −42.33 | −40.11 | -10.64 | -8.97 | +1.39 | +1.03 | 0 |

Taking the arithmetic mean value of the change rate of the first measurement and the second measurement mass concentration in Table 8, it can be seen that fly ash can increase the $Ca^{2+}$ mass concentration in tap water by 59.96% and can reduce the mass concentration of $Mg^{2+}$ by 41.22%, shale can increase the $Ca^{2+}$ mass concentration in tap water by 9.08% and reduce the $Mg^{2+}$ mass concentration by 9.805%, and clay can increase the $Ca^{2+}$ mass concentration in tap water by 4.81% and increase the $Mg^{2+}$ mass concentration by 1.21%.

## 4. DISCUSSION

Atmospheric pollutants include $NO_x$, $SO_2$, CO and are typically also are harmful to the human body. Among these, $NO_x$ and $SO_2$ are factors causing acid rain. In addition to pollutants, the greenhouse effect of unburned $CH_4$ far exceeds that of $CO_2$. Catalytic combustion can reduce $NO_x$, CO and $CH_4$ emissions, protect the environment and save natural gas. The catalytic combustion furnace has fast temperature rise and less pollution discharge.

When the three materials are heated to a certain temperature, the water molecules are separated, and many dense micropores are formed. According to the physical structure, the porous material has a large inner surface, and the molecules in the surface layer of the material have a molecular attraction to other small particles.

Clay, shale and fly ash sintered at 900°C have different effects on $Ca^{2+}$ and $Mg^{2+}$ in water. Among them, clay has the least influence on $Ca^{2+}$ and $Mg^{2+}$, while fly ash has the greatest influence, and shale has a moderate influence. All of the studied materials can increase the mass concentration of $Ca^{2+}$ in water, but fly ash had the greatest effect. Among the three materials, only clay can slightly increase the mass concentration of $Mg^{2+}$ in water, shale has a slight removal effect on $Mg^{2+}$ in water and fly ash has the greatest removal effect. Compared with general materials, the cost is low, and it is easily obtained. The findings of this research have to be seen in light of some limitations. Limited by experimental conditions, this experiment is only for fly ash, shale, and clay materials of specific origins, and the scope is limited, but the conclusion can be used as a reference for similar research. This research could be used as a reference for follow-up research to get more result.

## 5. CONCLUSIONS

Clay, shale and fly ash sintered at 900°C have different effects on $Ca^{2+}$ and $Mg^{2+}$ in water. Among them, clay has the least influence on $Ca^{2+}$ and $Mg^{2+}$, while fly ash has the greatest influence, and shale has a moderate influence. All of the studied materials can increase the mass concentration of $Ca^{2+}$ in water, but fly ash had the greatest effect. Among the three materials, only clay can slightly increase the mass

concentration of $Mg^{2+}$ in water, shale has a slight removal effect on $Mg^{2+}$ in water and fly ash has the greatest removal effect. Compared with general materials, the cost is low, and it is easily obtained.

The results show that fly ash from raw coal produced in Huaibei City of Anhui Province sintered at 900°C cannot reduce the hardness of tap water. However, this material can increase the mass concentration of $Ca^{2+}$ in water, which may be used in adsorbing $CO_2$ and $NH_3$ ( $Ca^{2+} + 2NH_3 + CO_2 + H_2O \rightarrow 2NH_4^+ + CaCO_3 \downarrow$ ). $CaCO_3$ can be recycled for medical treatment, materials and other fields. Calcium is an important part of plant cell walls and intercellular layers, and plays an important role in regulating the balance of physiological activities in plants. Deficiency in Ca element will lead to the death of new leaves and the atrophy of flowers. Moreover, $Ca^{2+}$ is involved in muscle contraction and nerve regulation in human bodies. Furthermore, $Ca^{2+}$ is also an important coagulation factor and participates in the coagulation process. Finally, $Ca^{2+}$ is also an important component of human bones. The lack of $Ca^{2+}$ will seriously affect the daily physiological activities of human body. Whether the high temperature modified fly ash can be used in the above fields needs to be further explored.

## ACKNOWLEDGEMENTS

This work was supported by the Beijing Municipality Key Lab of Heating Gas Supply Ventilating and Air Conditioning Engineering, Beijing Scholar Program and the Fundamental Research Funds for Beijing University of Civil Engineering and Architecture.

## NOMENCLATURE

| | |
|---|---|
| $r'$ | volume fraction (%) |
| $x_i$ | measured value of the *i*-th measurement (mg/L) |
| $\overline{x}$ | arithmetic means of a group of measuring values (mg/L) |
| $L$ | true value (mg/L) |

*Greek Symbols*

| | |
|---|---|
| $\Delta$ | absolute error (mg/L) |
| $\eta$ | rate of change (%) |
| $\rho$ | concentration (mg/L) |

## REFERENCES

Cao, X., Chu, Q., Song, X., Li, Y., Bian, J., 2019, "Flow characteristics of wet natural gas in different throttling devices," *Frontiers in Heat and Mass Transfer*, 13, 2.
http://dx.doi.org/10.5098/hmt.13.2

Chen, S., 2019, **"**Research on Influence of Fly Ash on Resistant Freezing Critical Strength of Concrete," *Contemporary Chemical Industry*, 12,2781-2784.
http://dx.doi.org/10.13840/j.cnki.cn21-1457/tq.2019.12.017

Chen, Z., Peng, W., Li, J., Liao, H., 2017, "Functional dissection and transport mechanism of magnesium in plants," *Seminars in Cell & Developmental Biology*, 8, 005.
http://dx.doi.org/10.1016/j.semcdb.2017.08.005

Dopont, V., Zhang, S., Williams, A., 2001, "Experiments and simulations of methane oxidation on a platinum surface," *Chemical Engineering Science*, 56, 2659-2670.
http://dx.doi.org/10.1016/S0009-2509(00)00536-4

Groll, G., "Energy and society: an overview", *Frontiers in Heat and Mass Transfer*, 15, 2.
http://dx.doi.org/10.5098/hmt.15.2

Huang, X., Zhao, H., Hu, X, Liu, F., Wang, L., Zhao, X., Gao, P., Ji, P., 2020, "Optimization of preparation technology for modified coal fly ash and its adsorption properties for $Cd^{2+}$," *Journal of Hazardous Materials*, 3, 392.
http://dx.doi.org/10.1016/j.jhazmat.2020.122461

Kobayashi, Y., Ogata, F., Saenjum, C., Nakamura, T., Kawasaki, N., 2020, "Removal of $Pb^{2+}$ from Aqueous Solutions Using K-Type Zeolite Synthesized from Coal Fly Ash," *Water*, 12, 2375.
http://dx.doi.org/10.3390/w12092375

Kuncoro, E.P., Fahmi, M.Z., 2013, "Removal of Hg and Pb in Aqueous Solution Using Coal Fly Ash Adsorbent," *Procedia Earth and Planetary Science*, 6, 377-382.
http://dx.doi.org/10.1016 / j.proeps.2013.01.049

Liu, R., Liu, W. *Gas combustion and combustion device,* 1st ed., CHINA MACHINE PRESS, No.22 Baiwanzhuang Street, Beijing, China.

Liu, Z., 2008, "Modification of ultra-fine coal fly ash and its thermodynamics of $Cr^{6+}$ adsorption". *Chemical Industry and Engineering Progress*, 4, 569-572+576.
http://dx.doi.org/10.3321/j.issn:1000-6613.2008.04.020

Luo, X., Yang, Y., Xu, D., 2020, "Study on adsorption of Cu(Ⅱ) by thermal modified fly ash," *Applied Chemical Industry*, 9, 2242-2245+2251.
http://dx.doi.org/10.16581/j.cnki.issn1671-3206.20200805.001

Medina-Ramirez, A.M., Gamero-Melo, P., Ruiz-Camacho, B., Minchaca-Mojica, J.I., Romero-Toledo, R., Gamero-Vega, K.Y., 2019, "Adsorption of Aqueous As (III) in Presence of Coexisting Ions by a Green Fe-Modified W Zeolite," *Water*, 11, 281.
http://dx.doi.org/10.3390/w11020281

Ministry of Ecological Environment of the People's Republic of China., 2020, "Annual report on prevention and control of solid waste pollution in large and medium sized cities in China 2019", http://www.mee.gov.cn/ywgz/gtfwyhxpgl/gtfw/201912/P020191231360445518365.pdf (accessed October 1, 2020)

Qi, X., Yang, M., Zhang, Y., 2017, "Numerical analysis of $NO_x$ production under the air staged combustion," *Frontiers in Heat and Mass Transfer*, 8, 3.
http://dx.doi.org/10.5098/hmt.8.3

Zhang, B., Li, J, Li, Y., Li, H., 2019, "Adsorption Characteristics of Several Bioretention-Modified Fillers for Phosphorus," *Water*, 10, 831.
http://dx.doi.org/10.3390/w10070831

Zhang, S., Xu, X., 2020, "Research on building glazed tile of fly ash added by radiation heat treatment inside catalytic combustion furnace of natural gas," *Frontiers in Heat and Mass Transfer*, 9, 14.
http://dx.doi.org/10.5098/hmt.14.9

Zhou, Y., Yang, H., Wang, L., Shi, Y., 2019, "Study on effect of quality of fly ash on concrete performance," *Concrete*, 12, 80-83.
http://dx.doi.org/10.3969/j.issn.1002-3550.2019.12.018